Electrochimica Acta 78 (2012) 11–16

Contents lists available at SciVerse ScienceDirect

Electrochimica Acta

journal homepage: www.elsevier.com/locate/electacta

Study on the cycling performance of $Li_4Ti_5O_{12}/LiCoO_2$ cells assembled with ionic liquid electrolytes containing an additive

Jin Hee Kim [a], Seo-youn Bae [a], Jeong-Hye Min [b], Seung-Wan Song [b,c,**], Dong-Won Kim [a,*]

[a] Department of Chemical Engineering, Hanyang University, Seungdong-Gu, Seoul 133-791, Republic of Korea
[b] Graduate School of Green Energy Technology, Chungnam National University, Daejeon 305-764, Republic of Korea
[c] Department of Fine Chemical Engineering & Applied Chemistry, Chungnam National University, Daejeon 305-764, Republic of Korea

ARTICLE INFO

Article history:
Received 27 January 2012
Received in revised form 3 May 2012
Accepted 3 May 2012
Available online 30 June 2012

Keywords:
Additive
Ionic liquid
Lithium-ion battery
Solid electrolyte interphase

ABSTRACT

The cycling behavior of $Li_4Ti_5O_{12}/LiCoO_2$ cells in the ionic liquid electrolytes based on 1-butyl-1-methylpyrrolidinium bis(trifluoromethanesulfonyl) imide (BMP-TFSI) with different additives, such as vinylene carbonate (VC), 1,3-propane sultone (PS) and their mixture is investigated. The cell assembled with BMP-TFSI containing 10 wt% VC/PS (1:1 by weight) exhibits reversible cycling behavior with good capacity retention. FTIR studies reveal that the electrochemically stable solid electrolyte interphase forms on $Li_4Ti_5O_{12}$ electrode in the presence of a mixture of VC and PS during cycling. The additives hardly affect the composition, thickness and stability of the surface film formed on the $LiCoO_2$ cathode.

1. Introduction

Lithium-ion batteries are used as power sources for portable electronic devices, due to their high energy density and long cycle life. Large-scale lithium-ion batteries for electric vehicles and energy storage systems have been investigated to achieve further technical developments. However, implementation of lithium-ion batteries for large capacity applications is still hindered by safety concerns, because the highly flammable organic solvents commonly used in lithium-ion batteries may cause fires or explosions during unpredictable events such as short circuits or local overheating. In the search for non-flammable electrolyte, ionic liquids have been recognized as one of the safest electrolytes, because they exhibit high thermal stability, non-flammability and negligible vapor pressure even at elevated temperatures [1–3]. Active materials such as lithium metal, carbon, $Li_4Ti_5O_{12}$, silicon and tin have been tested for use as anodes in ionic liquid electrolyte-based lithium batteries [4–18]. Among these materials, $Li_4Ti_5O_{12}$ is considered to be very promising, because it exhibits good reversibility with regard to the intercalation/deintercalation of lithium ions and shows no structural changes during charge–discharge cycling. Furthermore, the high operating voltage of $Li_4Ti_5O_{12}$ does not allow for the growth of lithium dendrites, and thus improvements in safety are expected. The electrochemical characteristics of $Li_4Ti_5O_{12}$ electrodes have been investigated in imidazolium-based ionic liquids due to their low viscosity and relatively high ionic conductivity [6,7]. Reale et al. reported the electrochemical behavior of $Li_4Ti_5O_{12}$ electrode in pyrrolidinium-based ionic liquids at 40 °C [14]. The ionic liquids in their work were found to be irreversibly decomposed on the electrode at a potential that was positive relative to that of Li/Li^+, which resulted in the formation of an unstable solid electrolyte interphase (SEI) on the electrode. Further, most ionic liquids exhibit low ionic conductivity compared to conventional liquid electrolytes. One way to solve these problems is to use a small amount of organic solvent as an additive [11,19–25], which forms an electrochemically stable SEI before reduction of the ionic liquid and also increases ionic conductivity by reducing the viscosity of the ionic liquid electrolyte. However, to our knowledge, there are few reports on the cycling behavior of $Li_4Ti_5O_{12}$-based lithium-ion batteries assembled with ionic liquid electrolytes containing an additive.

In the present work, the cycling behavior of $Li_4Ti_5O_{12}/LiCoO_2$ cells in ionic liquid electrolytes based on 1-butyl-1-methylpyrrolidinium bis(trifluoromethanesulfonyl) imide (BMP-TFSI) with different additives, such as vinylene carbonate (VC), 1,3-propane sultone (PS) and their mixture was investigated. These additives suppressed the reductive decomposition of ionic liquid electrolyte in the low potential region and thus allowed for a highly reversible capacity with stable cycling behavior. These beneficial properties were exploited for the development of a new type of lithium-ion battery with non-flammable ionic liquid electrolytes. The surface film formed on the $Li_4Ti_5O_{12}$ and $LiCoO_2$

* Corresponding author. Tel.: +82 2 2220 2337; fax: +82 2 2298 4101.
** Co-corresponding author.
E-mail addresses: swsong@cnu.ac.kr (S.-W. Song), dongwonkim@hanyang.ac.kr (D.-W. Kim).

0013-4686/$ – see front matter © 2012 Elsevier Ltd. All rights reserved.
http://dx.doi.org/10.1016/j.electacta.2012.05.161

electrode during cycling was also investigated by *ex situ* attenuated total reflection (ATR) FTIR spectroscopy.

2. Experimental

2.1. Preparation of ionic liquid electrolytes

BMP-TFSI was purchased from Chem Tech Research Incorporation and was used after drying under vacuum at 100 °C for 24 h. The water content in BMP-TFSI after drying was determined to be 8 ppm by Karl Fisher titration. VC and PS were purchased from Aldrich and dried over 4 Å molecular sieves before use. Ionic liquid electrolyte was prepared by dissolving 1.0 M lithium bis(trifluoromethanelsulfonyl) imide (LiTFSI, 3 M, highly purified reagent) in BMP-TFSI. The additive for forming SEI film such as VC, PS and VC/PS (1:1 by weight) was added to the ionic liquid electrolyte at a concentration of 10 wt%. The liquid electrolyte used for comparative purposes was 1.0 M $LiPF_6$ in ethylene carbonate (EC)/diethyl carbonate (DEC) (1:1 by volume, Techno Semichem Co., Ltd., battery grade). In order to improve the wettability of the separator for the ionic liquid electrolyte, poly(vinylidene fluoride-*co*-hexafluoropropylene) (P(VdF-co-HFP), Kynar 2801) was coated onto both sides of polyethylene separator (thickness: 25 μm, porosity: 40%), as described earlier [26]. The polymer-coated separator was easily wetted by the ionic liquid electrolytes containing a small amount of additive.

2.2. Electrode preparation and cell assembly

Anatase TiO_2 prepared by a hydrothermal method was used to synthesize the $Li_4Ti_5O_{12}$ [27]. High purity $TiCl_4$, urea and ammonium sulfate purchased from Aldrich were first mixed into a water–ethanol mixture submerged in an ice water bath. The mixed solution was transferred to a Teflon-lined autoclave and heated to 120 °C for 24 h. After incubation, the resulting slurry was filtered and washed with ethanol. The powder was vacuum-dried and sintered at 400 °C for 5 h in air. $Li_4Ti_5O_{12}$ was then synthesized from mesoporous anatase TiO_2 combined with Li_2CO_3 (molar ratio of Li/Ti is 0.4) and calcined at 900 °C for 20 h. The $Li_4Ti_5O_{12}$ electrodes were prepared by coating N-methyl pyrrolidone (NMP, Aldrich)-based slurry of $Li_4Ti_5O_{12}$, PVdF (Kureha Chemical Industry Co., Ltd.), super-P carbon (MMM Co.) and KS-6 carbon (Lonza) (80:10:5:5) onto copper foil. The cathode contained the same binder and super-P carbon along with $LiCoO_2$ active material (Japan Chemical), which was cast on aluminum foil. The average mass of active $Li_4Ti_5O_{12}$ and $LiCoO_2$ materials in the electrodes were about 8.0 and 6.9 mg cm^{-2}, respectively. All of the electrodes were roll pressed to enhance particulate contact and adhesion to foils. The coin-type $Li_4Ti_5O_{12}/LiCoO_2$ cell (CR2032) was assembled by setting two electrodes face to face, with a polymer-coated separator inserted between them. All cell assembly was carried out in an argon-filled glove box. After the cell assembly process, the cells were kept at 55 °C for 24 h to imbue the electrode with the ionic liquid electrolyte solution.

2.3. Measurements

A three-electrode cell was used for linear sweep voltammetry (LSV) measurements with a stainless steel as working electrode and lithium foil as counter and reference electrodes. A scanning rate was 1.0 mV s^{-1} in the LSV experiments. Charge and discharge cycling tests of the cells were conducted with battery testing equipment (WBCS 3000, Wonatech) at a constant current density of 0.2 mA cm^{-2} (0.2 C rate) after two preconditioning cycles at a 0.1 C rate, over a voltage range of 1.6–2.7 V at 55 °C. For differential scanning calorimetry (DSC) experiments, the cells were fully charged to 2.7 V after 100 cycles and were disassembled in the dry box. Approximately 5 mg of the cathode scraped from the current collector was hermetically sealed in a stainless steel pan, and measurements were taken at a heating rate of 1 °C min^{-1}. Surface characterization of the $Li_4Ti_5O_{12}$ and $LiCoO_2$ electrode before and after cycles in different electrolytes was conducted by *ex situ* ATR FTIR spectroscopy using an IR spectrometer (Nicolet 6700) equipped with a mercury–cadmium–telluride detector. Residual electrolyte components were removed from the electrode by washing it thoroughly with dimethyl carbonate prior to collecting the FTIR data. Since the electrodes were directly mounted on a closed single-reflection ATR unit with a Ge optic in an Ar-filled glove box, there was no atmospheric contamination of the samples during transportation to the IR instrument or during the IR measurement. In order to investigate the flammable behavior of ionic liquid electrolyte solution, an inert glass-fiber wick (3 cm × 3 cm) was soaked with the electrolyte solution, and it was ignited with flame source for 10 s. The electrolyte was judged to be non-flammable if the electrolyte never ignited during the testing, or if the ignition of electrolyte ceased when the flame source was removed [28].

3. Results and discussion

The electrochemical stability of the ionic liquid electrolytes containing different additives was investigated through LSV measurements, and the results are shown in Fig. 1. It is observed in Fig. 1(a) that the cathodic current starts to increase around 1.5 V *vs.* Li/Li^+ in the ionic liquid electrolyte without additive. Since lithium deposition should have occurred around 0 V, the observed cathodic current may correspond to the reductive decomposition of the ionic liquid electrolyte. The measured value of the reductive decomposition is in good agreement with that observed in a LiTFSI and 1-butyl-1-ethylpyrrolidinium bis(trifluoromethanesulfonyl) imide solution [14]. For the ionic liquid electrolyte with additive, reduction of additives takes place at a potential that is more positive than that of ionic liquid electrolyte, resulting in the formation of a SEI film on the electrode. The SEI film may prevent further reductive decomposition of the ionic liquid electrolyte and kinetically extends the cathodic stability to 0 V *vs.* Li/Li^+. It should be noted that the reductive decomposition of ionic liquid electrolyte can hardly be observed when a mixture of VC and PS is used. In the anodic scan shown in Fig. 1(b), the oxidative decomposition occurs above 5.0 V in the ionic liquid electrolyte without additive. The addition of VC, PS and VC/PS decreases the anodic stability of electrolyte solution, which may originate from the anodic decomposition of the additive. Nevertheless, they show high anodic stability higher than 4.7 V, which is suitable for allowing the electrochemical operation of $Li_4Ti_5O_{12}/LiCoO_2$ cells considered in the present study.

Fig. 2 shows the charge and discharge curves of the $Li_4Ti_5O_{12}/LiCoO_2$ cells in ionic liquid electrolyte with and without additive, which are obtained for initial preconditioning cycles over a voltage range of 1.6–2.7 V at a 0.1 C rate. The large irreversible capacity is usually observed during initial cycles in the lithium-ion cells, which arises from the formation of SEI on the surface of the negative electrode. Thus the first and second cycles are referred to as preconditioning cycle in this study. The discharge capacities obtained during the first preconditioning cycle range from 106 to 120 mAh g^{-1} based on $LiCoO_2$ active material in the cathode. The irreversible capacity loss for the first cycle increases when the additives are used. The initial large irreversible capacity of the cell with additive can be attributed to the reduction of additive, resulting in the formation of SEI layer on the $Li_4Ti_5O_{12}$ electrode. Nakagawa et al. also reported large

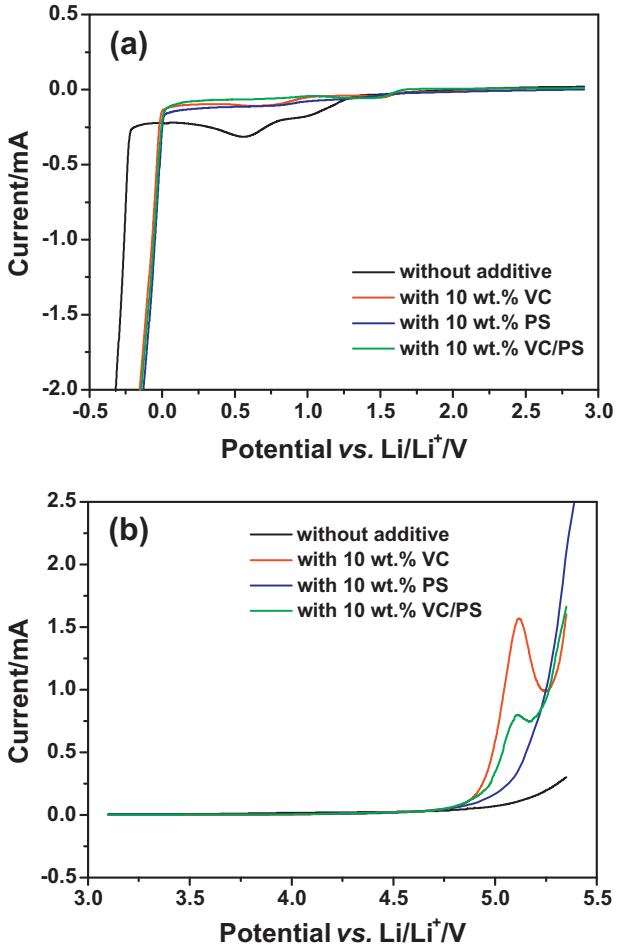

Fig. 1. Linear sweep voltammograms of ionic liquid electrolyte without and with additive (scan rate: 1 mV s^{-1}): (a) cathodic scan and (b) anodic scan.

irreversible capacity (24.3–34.0%) in the $Li_4Ti_5O_{12}/LiCoO_2$ cells assembled with 1-ethyl-3-methylimidazolium tetrafluoroborate-based ionic liquid electrolytes at a constant current density of 0.025 mA cm^{-2}, which may be caused by production of a passivation layer due to the side reactions in anode interface [29]. For the second cycle, however, the cells with additive exhibit a lower irreversible capacity loss than that of cell without additive. The coulombic efficiencies for the second cycle are 92.1, 94.2, 92.9 and 96.2% for the cell without additive and with VC, PS and VC/PS, respectively. The initial irreversible reaction observed around 2.0 V for the first cycle in the cell with VC-containing ionic liquid electrolyte (Fig. 2(b) and (d)) disappears for the second charging cycle. These results suggest that the SEI layer formed on the $Li_4Ti_5O_{12}$ electrode during the first cycle effectively suppresses further reduction of ionic liquid electrolyte during the second cycle, which leads to a reduction in the irreversible capacity loss after the first cycle.

After two preconditioning cycles, the cells were cycled over the same cut-off voltage at a 0.2 C rate. Fig. 3(a) shows the charge and discharge curves of the 1st, 10th, 20th, 50th and 100th cycles of the $Li_4Ti_5O_{12}/LiCoO_2$ cell assembled with ionic liquid electrolyte containing 10 wt% VC/PS (1:1 by weight). The cell had an initial discharge capacity of 111.1 mAh g^{-1}, which declined to 96.2 mAh g^{-1} after 100 cycles, while the cycling efficiency steadily increased with cycle number. Fig. 3(b) shows the discharge capacities as a function of cycle number in the cells prepared with ionic liquid electrolyte containing different additives. It is clear that the cycling characteristics of cells are dependent on the type of additives used. The initial discharge capacity is the lowest in the cell prepared with ionic liquid electrolyte without additive, which is due to the fact that the use of a highly viscous ionic liquid electrolyte causes increases in both electrolyte resistance and charge transfer resistance at the electrode/electrolyte interface. On the other hand, the addition of VC, PS and VC/PS increases the initial discharge capacity. Such an increase can be attributed to both an enhancement in the ionic conductivity of the electrolyte and effective penetration of the electrolyte into the electrodes. With respect to capacity retention, the cell in an ionic liquid electrolyte without additive showed significant capacity fading during cycling, which may be related to undesirable and irreversible decomposition reactions of the ionic liquid electrolyte during cycling. In contrast, the addition of VC, PS or VC/PS to ionic liquid electrolyte leads to improved discharge capacity retention, which results from the formation of an electrochemically stable SEI layer on the $Li_4Ti_5O_{12}$ electrode during repeated cycling.

Rate capability of the $Li_4Ti_5O_{12}/LiCoO_2$ cells in ionic liquid electrolytes containing different additives was evaluated. Before the execution of the rate capability test, the cells were initially cycled 10 times at a low current rate (0.1 C rate) in order to induce the formation of an SEI layer on the electrode. The cells were then charged to 2.7 V at a constant current of 0.2 C and discharged at different current rates ranging from 0.2 to 2.0 C. The discharge curves of the $Li_4Ti_5O_{12}/LiCoO_2$ cell assembled with ionic liquid electrolyte containing VC/PS are given in Fig. 4(a). Cycling performance at 1.0 C rate, with a capacity of 105.1 mAh g^{-1}, is considered good. However, the discharge capacity abruptly decreased to 73.6 mAh g^{-1} at 2.0 C rate, which can be attributed to the high resistance of electrolyte. Fig. 4(b) compares the rate capabilities of the $Li_4Ti_5O_{12}/LiCoO_2$ cells assembled with ionic liquid electrolytes containing different additives. In this figure, the relative capacity is defined as the ratio of the discharge capacity at a specific C rate to the discharge capacity delivered at the 0.2 C rate. The results showed that the type of additive used affected high rate performance. As expected, the cell prepared with ionic liquid electrolyte without additive exhibited the lowest high rate performance, while the relative capacity at 2.0 C rate was the highest when a mixture of VC and PS was added to the ionic liquid electrolyte. This suggests that the SEI film formed in the presence of VC/PS may be uniform and stable enough to provide favorable interfacial charge transport kinetics.

In order to investigate the composition of surface film formed on $Li_4Ti_5O_{12}$ anodes and $LiCoO_2$ cathodes in ionic liquid electrolytes with and without additives, the electrodes were analyzed after 100 cycles using *ex situ* ATR FTIR spectroscopy. Fig. 5 shows the IR spectra of the $Li_4Ti_5O_{12}$ electrodes cycled in the different electrolytes. The surface of a pristine electrode (Fig. 5(a)) exhibits peaks that originated from the PVdF binder [30]. Overall, the surfaces of the cycled electrodes show clearly new peaks that can be distinguished from those of PVdF. First, the electrode cycled in ionic liquid electrolyte without additive exhibits tiny new peaks at 1654, 1618, 1456, 1330 and near 837 cm^{-1}, which are attributed to the ν(C=O) from alkyl carbonate salt $-OCO_2^-M^{n+}$ (M = Li/Ti) and carboxylate salt $-CO_2^-M^{n+}$, respectively [31]. Strong and broad new peaks appearing near 1512–1430 cm^{-1} are attributed to the $\nu(CO)_{sym}$ and $\nu(CO)_{asym}$ of Li_2CO_3. The Li_2CO_3 and low concentration organic species may be the decomposition products of BMP cations combined with oxygen from $Li_4Ti_5O_{12}$ and TFSI anions. Tiny peaks near 1350, 1330 and 879 cm^{-1} are attributed to $\nu(-SO_2-)$, and those at 1230–1180 and 752 cm^{-1} to ν(C—F) and ν(C—F), respectively, are attributed to TFSI decomposition products [32]. For the electrode cycled in the presence of VC additive, new prominent peaks of the CH_3-CH_2 alkyl group appear in the region 2950–2850 and 1456–1443 cm^{-1}, which are due to new surface compounds, as well as peaks due to Li_2CO_3 and TFSI decomposition products. Strong

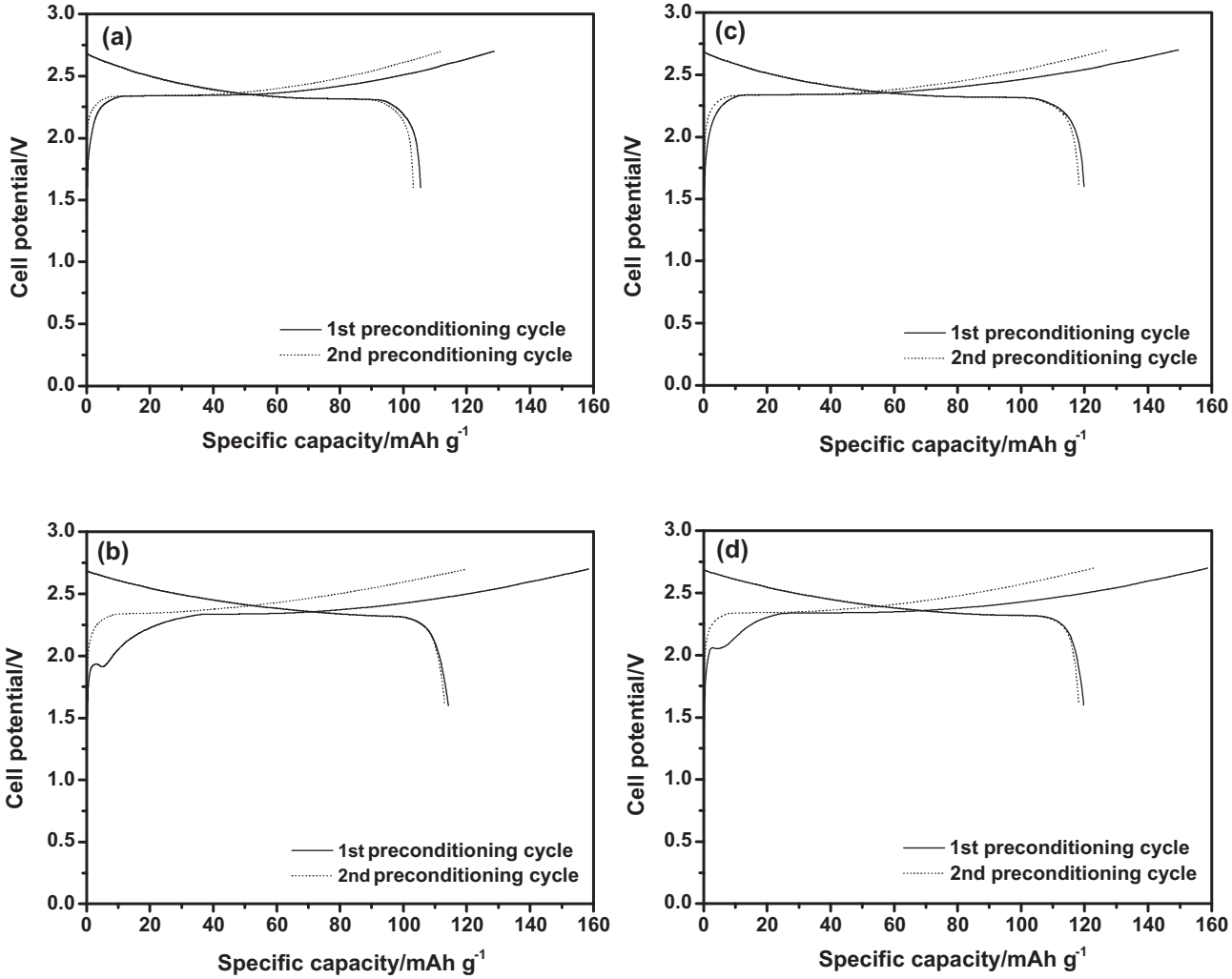

Fig. 2. Charge and discharge curves of $Li_4Ti_5O_{12}/LiCoO_2$ cells in ionic liquid electrolyte with and without additive, which are obtained for initial preconditioning cycles (55 °C, 0.1 C rate). (a) Without additive, (b) with VC, (c) with PS and (d) with VC/PS.

absorbance of the alkyl group indicates the surface compounds to be polymeric [33]. Prominent peaks at 1806 and 1741 cm^{-1} are due to ν(C═O) of carboxylic acid anhydride —CO—O—CO— and the one at 1776 cm^{-1} to an ester —CO_2R group, respectively. Two shoulders at 1270 and 1072 cm^{-1}, due to ν(C—O—C) and ν(O—C—C), respectively, confirm the presence of ester compounds. Other new peaks at 1612 and 1583 cm^{-1} are attributed to ν(C═O) of carboxylate salts. The presence of such polymeric/organic compounds is direct evidence of VC decomposition. The electrode surface cycled in PS exhibits a lower absorbance spectrum than that cycled in VC, probably due to the lower concentration of surface species. Newly observed peaks at 1228, 1072 and 991 cm^{-1}, which overlap with the peaks of ν(C—F), are attributed to $\nu(SO_2)_{asym}$ and $\nu(SO_2)_{sym}$, respectively, of alkyl sulphate salt R-$SO_4^-M^+$, and/or $\nu(SO_3)_{asym}$ and $\nu(SO_3)_{sym}$ of sulphonic salt $SO_3^-M^+$. In the presence of VC and PS, the cycled electrode surface shows all of the prominent peaks that are observed in Fig. 5(c) and (d). In particular, significant enhancement of peak absorbance at 1228 cm^{-1} indicates a further increase in the concentration of SO_2-containing inorganic salt. These results indicate that in the presence of VC and PS together, the surface of cycled $Li_4Ti_5O_{12}$ is more effectively covered by a thicker layer than with other electrolyte composition. When VC and PS are added to ionic liquid electrolyte together, the electrode surface consists of a mixture of polymeric/organic and inorganic salt surface species together at a relatively high concentration level. The presence of these compounds provides a more stable surface layer, which results in good cycling performance.

Fig. 6 shows the IR spectra of the $LiCoO_2$ cathodes cycled in the different electrolytes. Overall the spectral feature of all cycled cathodes is the almost same with each other. Observation of strong prominent peaks of the PVdF binder reflects that the surface layer is very thin and the coverage of surface compounds is low. All the cycled $LiCoO_2$ cathodes clearly exhibit a new peak around 3404 cm^{-1}, which is attributed to ν(NH) of secondary amine. A broad peak ranged from 1512 to 1430 cm^{-1} is attributed to the Li_2CO_3. Strong new peaks at 1394 and 1374 cm^{-1} are attributed to the $\nu(-SO_2-)_{asym}$ from SO_2-containing compounds. Peaks at 1272 and 788 cm^{-1} are ascribed to ν(C—F) and ≐(C—F). The presence of —SO_2— and C—F signatures are of the decomposition products of TFSI anion [32]. No clear evidence for the effect of additives on the $LiCoO_2$ cathode is observed, as expected in Fig. 1(b). It is thus believed that the additives in the ionic liquid electrolyte strongly affect on the surface layer of $Li_4Ti_5O_{12}$ anode in the aspects of the composition, thickness and stability, but not on that of the $LiCoO_2$ cathode.

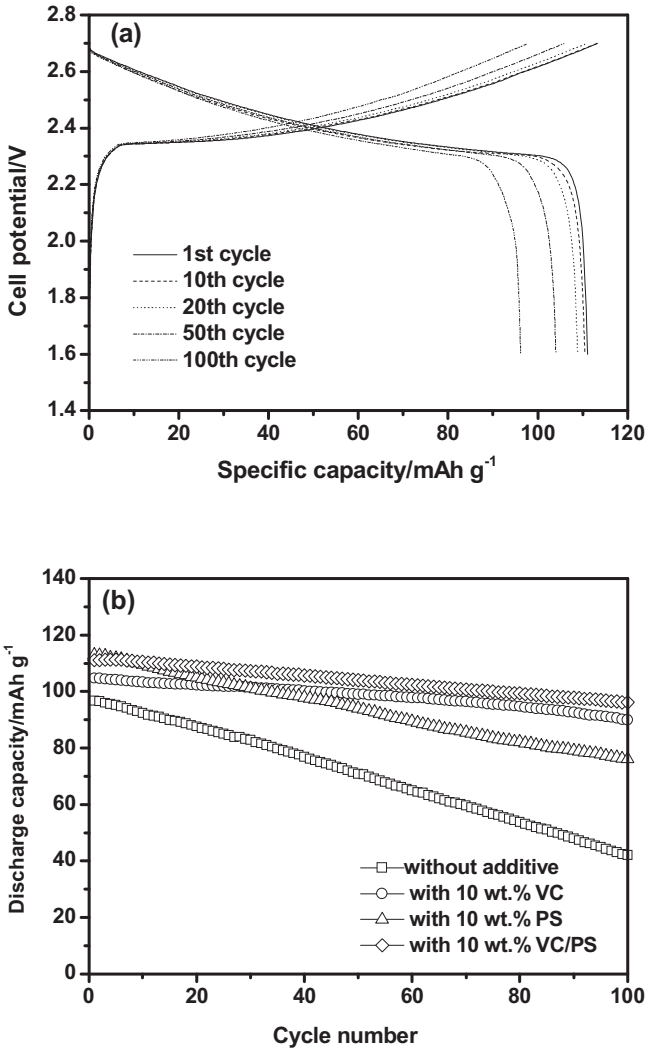

Fig. 3. (a) Charge and discharge curves of the $Li_4Ti_5O_{12}/LiCoO_2$ cell in ionic liquid electrolyte containing 10 wt% VC/PS, and (b) discharge capacities as a function of the cycle number for cells with different additives (55 °C, 0.2 C rate).

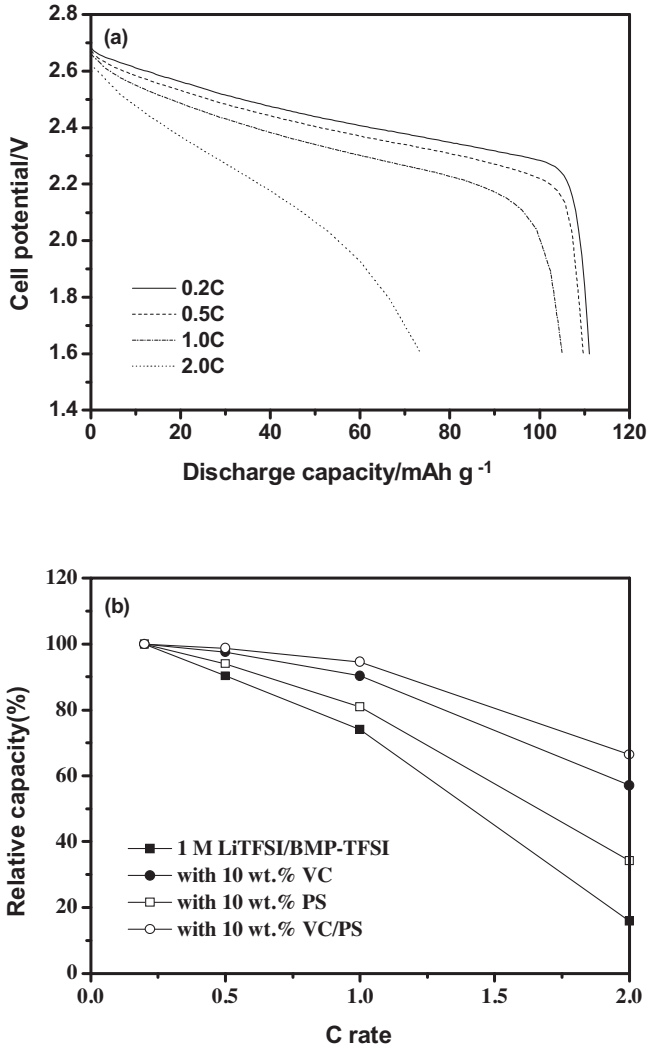

Fig. 4. (a) Discharge profiles of the $Li_4Ti_5O_{12}/LiCoO_2$ cell in ionic liquid electrolyte containing 10 wt% VC/PS, and (b) relative capacities of the cells with different additives as a function of C rate.

The flammability of the ionic liquid electrolyte containing different additives was investigated. None of the ionic liquid electrolytes with or without additives showed any combustion, even during ignition with a flame source, which means all the ionic liquid electrolytes are non-flammable. Thermal stability of the delithiated cathode materials is also of great importance for battery safety. DSC measurements were performed to evaluate the thermal stability of the cathode material in a fully charged state. Fig. 7 shows the DSC profiles of the cathode materials charged to 2.7 V, which are obtained after 100 cycles. For the purpose of comparison, the DSC trace of $Li_{1-x}CoO_2$ cycled in standard liquid electrolyte (1.0 M $LiPF_6$ in EC/DEC) is also included in the figure. The $Li_{1-x}CoO_2$ material cycled in standard liquid electrolyte has a large exothermic peak with a reaction heat of 466.6 J g^{-1} at 244.6 °C, which arises from the reaction of organic solvents with the oxygen released from the charged $Li_{1-x}CoO_2$ material [34–36]. On the other hand, the $Li_{1-x}CoO_2$ material in the cell assembled with ionic liquid electrolyte has a much smaller exothermic reaction peak (141.5 J g^{-1}) at a higher temperature (285.2 °C). These results suggest that the delithiated $Li_{1-x}CoO_2$ material is less reactive toward the ionic liquid electrolyte, leading to an improvement in thermal stability. The addition of VC, PS and VC/PS does not significantly affect the thermal stability of the cathode material, as shown in the figure, which

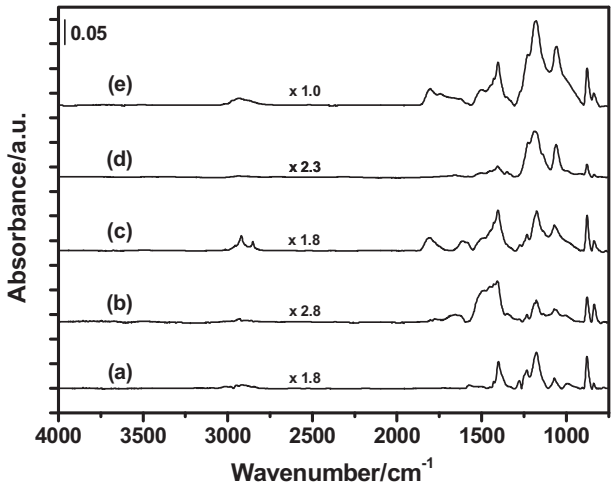

Fig. 5. FTIR spectral comparison of a pristine $Li_4Ti_5O_{12}$ anode and $Li_4Ti_5O_{12}$ anodes cycled in ionic liquid electrolytes containing different additives. (a) A pristine electrode, (b) an electrode cycled in ionic liquid electrolyte without additive, and electrodes cycled in ionic liquid electrolyte with (c) VC, (d) PS, and (e) VC/PS.

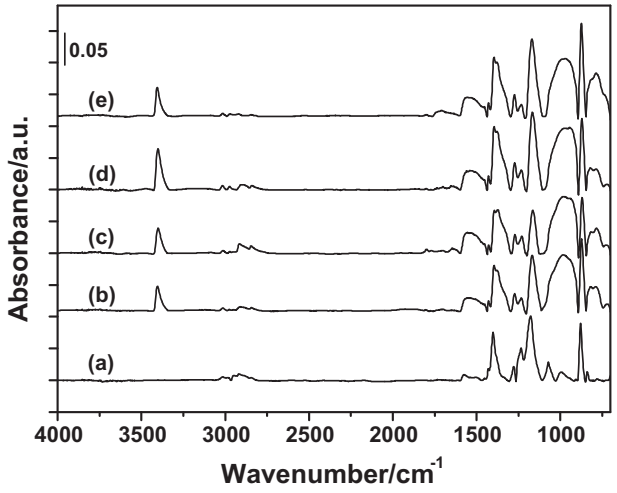

Fig. 6. FTIR spectral comparison of a pristine $LiCoO_2$ cathode and $LiCoO_2$ cathodes cycled in ionic liquid electrolytes containing different additives. (a) A pristine electrode, (b) an electrode cycled in ionic liquid electrolyte without additive, and electrodes cycled in ionic liquid electrolyte with (c) VC, (d) PS, and (e) VC/PS.

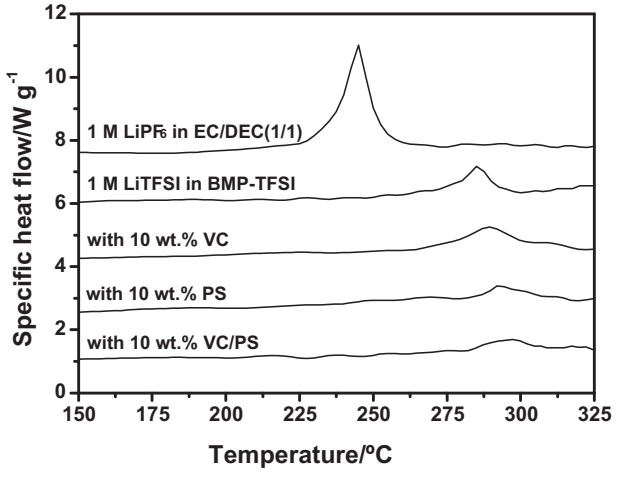

Fig. 7. DSC profiles of $Li_{1-x}CoO_2$ cathode materials charged to 2.7 V after 100 cycles in cells assembled with ionic liquid electrolytes containing different additives.

indicates that the thermal stability of the cathode material is maintained in the presence of an ionic liquid electrolyte with a small amount of additive.

4. Conclusions

The cycling behavior of $Li_4Ti_5O_{12}/LiCoO_2$ cells in ionic liquid-based electrolytes composed of BMP-TFSI and a small amount of organic additive was investigated. The addition of organic solvents suppressed the reductive decomposition of BMP-TFSI. The $Li_4Ti_5O_{12}/LiCoO_2$ cell in BMP-TFSI containing a mixture of VC and PS exhibited high discharge capacity and good capacity retention. Surface characterization of the $Li_4Ti_5O_{12}$ electrode with FTIR analysis confirmed that a stable and thick surface layer was formed on the electrode during cycling when a mixture of VC and PS was added to the ionic liquid electrolyte. The addition of VC, PS and VC/PS hardly affected the surface layer of $LiCoO_2$ cathode during cycling.

Acknowledgments

This work was supported by the IT R&D program of MKE/KEIT (KI002176-2010-02) and the National Research Foundation (NRF) of Korea Grant funded by the Korea government (MEST) (NRF-2009-C1AAA001-0093307). This work was partly supported by the Human Resources Development of the KETEP grant funded by the Korea government Ministry of Knowledge Economy (No. 20104010100560).

References

[1] M. Galinski, A. Lewandowski, I. Stepniak, Electrochimica Acta 51 (2006) 5567.
[2] M. Armand, F. Endres, D.R. MacFarlane, H. Ohno, B. Scrosati, Nature Materials 9 (2009) 621.
[3] A. Lewandowski, A. Swiderska-Mocek, Journal of Power Sources 194 (2009) 601.
[4] M. Egashira, S. Okada, J.-I. Yamaki, D.A. Dri, F. Bonadies, B. Scrosati, Journal of Power Sources 138 (2004) 240.
[5] B. Garcia, S. Lavallee, G. Perron, C. Michot, M. Armand, Electrochimica Acta 49 (2004) 4583.
[6] A. Chagnes, M. Diaw, B. Carre, P. Willmann, D. Lemordant, Journal of Power Sources 145 (2005) 82.
[7] M. Holzapfel, C. Jost, A. Prodi-Schwab, F. Krumeich, A. Wursig, H. Buqa, P. Novak, Carbon 43 (2005) 1488.
[8] H. Zheng, K. Jiang, T. Abe, Z. Ogumi, Carbon 44 (2006) 203.
[9] M. Ishikawa, T. Sugimoto, M. Kikuta, E. Ishiko, M. Kono, Journal of Power Sources 162 (2006) 658.
[10] H. Sakaebe, H. Matsumoto, K. Tatsumi, Electrochimica Acta 53 (2007) 1048.
[11] A. Lewandowski, A. Swiderska-Mocek, Journal of Power Sources 171 (2007) 938.
[12] L. Zhao, J.-I. Yamaki, M. Egashira, Journal of Power Sources 174 (2007) 352.
[13] M. Taggougui, M. Diaw, B. Carre, P. Willmann, D. Lemordant, Electrochimica Acta 53 (2008) 5496.
[14] P. Reale, A. Fernicola, B. Scrosati, Journal of Power Sources 194 (2009) 182.
[15] J. Hassoun, A. Fernicola, M.A. Navarra, S. Panero, B. Scrosati, Journal of Power Sources 195 (2010) 574.
[16] C.C. Nguyen, S.W. Song, Electrochemistry Communications 12 (2010) 1593.
[17] N.S. Choi, Y. Lee, S.S. Kim, S.C. Shin, Y.M. Kang, Journal of Power Sources 195 (2010) 2368.
[18] J.A. Choi, D.W. Kim, Y.S. Bae, S.W. Song, S.H. Hong, S.M. Lee, Electrochimica Acta 56 (2011) 9818.
[19] M. Herstedt, A.M. Andersson, H. Rensmo, H. Siegbahn, K. Edstrom, Electrochimica Acta 49 (2004) 4939.
[20] T. Sato, T. Maruo, S. Marukane, K. Takagi, Journal of Power Sources 138 (2004) 253.
[21] S.S. Zhang, Journal of Power Sources 162 (2006) 1379.
[22] X. Zuo, M. Xu, W. Li, D. Su, J. Liu, Electrochemical Solid-State Letters 9 (2006) A196.
[23] G. Park, H. Nakamura, Y. Lee, M. Yoshio, Journal of Power Sources 189 (2009) 602.
[24] M. Xu, W. Li, B.L. Lucht, Journal of Power Sources 193 (2009) 804.
[25] A. Orita, K. Kamijima, M. Yoshida, K. Dokko, M. Watanabe, Journal of Power Sources 196 (2011) 3874.
[26] S.M. Eo, E. Cha, D.W. Kim, Journal of Power Sources 189 (2009) 766.
[27] H.G. Jung, C.S. Yoon, J. Prakash, Y.K. Sun, Journal of Physical Chemistry C 113 (2009) 113.
[28] H. Nakagawa, Y. Fujino, S. Kozono, Y. Katayama, T. Nukuda, H. Sakaebe, H. Matsumoto, K. Tatsumi, Journal of Power Sources 174 (2007) 1021.
[29] H. Nakagawa, S. Izuchi, K. Kuwana, T. Nukuda, Y. Aihara, Journal of the Electrochemical Society 150 (2003) A695.
[30] S.W. Song, G.V. Zhuang, P.N. Ross, Journal of the Electrochemical Society 151 (2004) A1162.
[31] G. Socrates, Infrared Characteristic Group Frequencies, Tables and Charts, 2nd ed., John Wiley & Sons, New York, USA, 1994.
[32] P.C. Howlett, N. Brack, A.F. Hollenkamp, M. Forsyth, D.R. MacFarlane, Journal of the Electrochemical Society 153 (2006) A595.
[33] Y. Wang, S. Nakamura, K. Tasaki, P.B. Balbuena, Journal of the American Chemical Society 124 (2002) 4408.
[34] J.R. Dahn, E.W. Fuller, M. Obrovac, U. von Sacken, Solid State Ionics 69 (1994) 265.
[35] D.D. MacNeil, J.R. Dahn, Journal of the Electrochemical Society 148 (2001) A1205.
[36] Y. Baba, S. Okada, J.-I. Yamaki, Solid State Ionics 148 (2002) 311.